Fine-Structure and Physical Properties of Polyethylene Fibers in High-Speed Spinning. I. Effect of Melt-Flow Rate in the High-Density Polyethylene

H. H. CHO,[1] K. H. KIM,[1] H. ITO,[2] T. KIKUTANI[2]

[1] Department of Textile Engineering, Pusan National University, Pusan 609-735, South Korea

[2] Department of Organic and Polymeric Materials, Tokyo Institute of Technology, 2-12-1, O-okayama, Meguro-ku, Tokyo 152, Japan

Received 24 May 1999; accepted 29 October 1999

ABSTRACT: High-density polyethylene (HDPE) fibers, obtained from a melt-flow rate (g/10 min) of 11 and 28, was produced by a high-speed melt-spinning method in the range of take-up velocity from 1 to 8 km/min and from 1 to 6 km/min, respectively. The change of fiber structure and physical properties with increasing take-up velocity was investigated through birefringence, wide-angle X-ray diffraction (WAXD), differential scanning calorimetry (DSC), a Rheovibron, and a Fafegraph-M. With an increase in take-up velocity, the birefringence showed a sigmoidal increase, which has distinct changes in the range of 1–5 km/min. Throughout the whole take-up velocities, the birefringence of HDPE(11) was higher than that of HDPE(28). With increasing take-up velocity, the crystalline orientation was transformed from a-axis orientation to c-axis orientation. These crystalline relaxations are confirmed by the tan δ peak of high-speed spun HDPE fibers. The intensity of the crystalline relaxation peak decreases with increasing take-up velocity in both HDPE(11) and HDPE(28). As above, the crystalline relaxation peaks shift to lower temperature with increasing take-up velocity. With increasing take-up velocity, the ultimate strain decreases while both specific stress and the initial modulus increase. The mechanical behavior may be closely related to, as investigated by birefringence, orientation of the amorphous region, etc., the take-up velocity. © 2000 John Wiley & Sons, Inc. J Appl Polym Sci 77: 1182–1195, 2000

Key words: high-speed spinning; high-density polyethylene (HDPE); crystalline orientation; crystalline relaxation

INTRODUCTION

High-speed spinning, as a part of melt spinning, is an ideal and attractive process which can fully satisfy such requirements as the saving of energy, reduction of labor, and simplification of industrial operations. The characteristics of the obtained fibers from this process have been of interest; that is, the fibers produced by high-speed spinning have had low shrinkage and high tenacity. An attempt of high-speed spinning was begun in the 1940s. In 1952, DuPont a registered U.S. patent. In the 1970s, the take-up velocities became higher with improvement in the winding technology. In 1971, Ueda et al.[1] reported the relationship between the take-up velocity and structure formation of nylon 6 fiber. Further, since the late 1970s, many studies have been reported on high-speed spinning of polyamide and PET.[2–10] The spinning velocity of 1400 m/min has been

Correspondence to: H. H. Cho.

Journal of Applied Polymer Science, Vol. 77, 1182–1195 (2000)

achieved in PET. Academic studies on high-speed spinning of PET and nylon, therefore, have been done for a long time. As for polyolefin, Shimizu et al.[11] reported on high-speed spinning to 7 km/min of polypropylene, and as the take-up velocity increased, the degree of crystallinity and birefringence of as-spun fiber enormously increased, and at the take-up velocities higher than 2 km/min, they showed leveling off at about 60% and 25 $\times 10^{-3}$.

For polyethylene,[12] on the other hand, it is known that it is difficult to adapt it for high-speed spinning because of rapid crystallization, and in the spinning velocity of 1 km/min, the mechanical properties become mostly uniformed but the crystal orientation is higher. White[13] investigated the structures and the physical properties of both HDPE and LDPE at take-up velocities of 1 km/min and below. With further crystal orientation, the b-axis is perpendicular to the fiber axis, and the c-axis is parallel to the fiber axis and then the a- and b-axis is perpendicular to the fiber axis. Dees and Spruiell[14] proposed a mechanism of crystallization and orientation with increasing take-up velocity for melt-spun HDPE. Further increase in take-up velocity beyond the point at which significant row nucleation first occurs causes the cooling rate to increase rapidly enough to suppress the crystallization temperature, in spite of any additional increase in crystallization rates caused by increased spinline stresses. Crystallization under these conditions results in smaller interlamellar spacings (long periods). However, for the production of nonwoven fabrics, high-speed spinning has been required. In the present study, the fine-structure formation and physical properties of high-speed spun HDPE polymers having different melt flow rates were investigated.

EXPERIMENTAL

High-Speed Spinning

A gear pump was used for the precise control of the mass-flow rate in the extruder. HDPE polymers were extruded from a spinneret with a single hole of 0.5-mm diameter at 220°C. The melt-flow rates (MFR, g/10 min) of the HDPE samples was 11 and 28. The mass-flow rate was controlled to 5.0 g/min. In this study, quenching air was not applied to the spinning line. The polymer extruded from the spinneret was taken up by a high-speed winder placed at 330 cm below the spinning head. The take-up velocities of HDPE(11) and HDPE(28) were 1–8 and 1–6 km/min, respectively.

Molecular Weight Distribution

Average molecular weights ($\bar{M}_n$, $\bar{M}_w$) and the molecular weight distribution (MWD = $\bar{M}_w/\bar{M}_n$) of the polymer samples used were determined using a gel permeation chromatograph of Waters GPS-150C with 1,2,4-trichlorobenzene as a solvent at 140°C. Monodisperse polystyrene standards were used for the universal calibration.

Rheological Property

The rheological property was investigated at 220°C (corresponding to the spinning temperature) using a Physica US 200, which has a parallel-plate geometry, for the dynamic test. The frequency range was 1–100 rad/s. The diameter and the thickness of the sample were 25 and 1.6 mm, respectively.

Birefringence

The birefringence with take-up velocities was measured using an interference microscope equipped with a polarizing filter placed on parallel and perpendicular directions to fiber axis. The standard refractive liquid was used for the immersion liquid, and the refractive indices of the immersion liquids were measured by an Abbe refractive apparatus.

The schematic of the refractive fringe for the fiber obtained by an interference microscope is shown in Figure 1. The shift of the fringe (d) measured with the interference microscope is proportional to the product of the thickness ($2y$) and the refractive index difference between the immersion liquid (N) and the sample (n). The length between fringes is D in eq. (1) and λ is the wavelength of the incident light. Birefringence (Δn) was calculated from two refractive indices which are parallel ($n_{\parallel}$) and perpendicular ($n_{\perp}$) to the fiber axis, respectively:

$$\frac{d}{D}\lambda = (n - N)2y \tag{1}$$

$$\Delta n = n_{\parallel} - n_{\perp} \tag{2}$$

Density and Crystallinity

Density was measured by the density gradient method using carbon tetrachloride (specific grav-

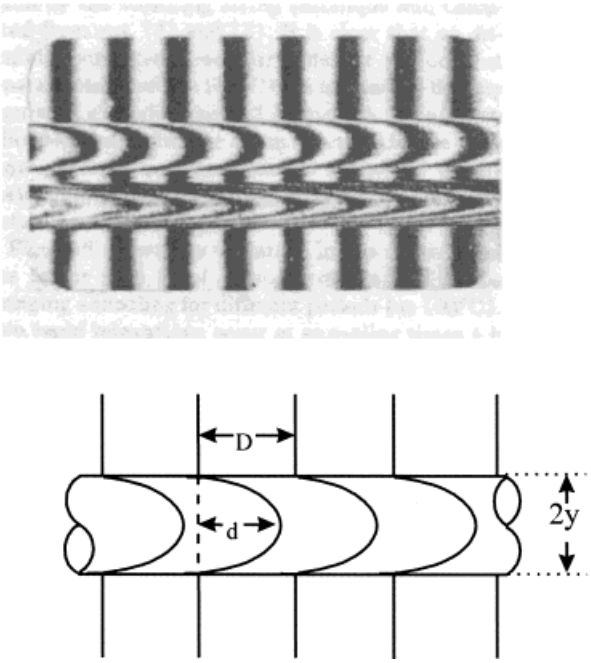

Figure 1 Schematic of fringe pattern for fiber observed under an interference microscope.

ity: 1.59) and *n*-heptane (0.68) at 23°C. The weight crystallinity (χ_c) was calculated by eq. (3) from the measured density (ρ). The values of 1.00 and 0.855 were used as the crystalline density (ρ_c) and amorphous density (ρ_a), respectively[15]:

$$\chi_c(\%) = \frac{\rho_c(\rho - \rho_a)}{\rho(\rho_c - \rho_a)} \tag{3}$$

X-ray Diffraction

Equatorial X-ray diffraction profiles were obtained by a Rigaku X-ray diffractometer of D/max-III-A type with CuKα radiation through a Ni filter. Crystalline orientation was estimated by the azimuthal intensity distribution of well-resolved wide-angle X-ray reflection lines of the (200) and (020) planes. Orientation functions for the *a*-axis and *b*-axis of polyethylene crystals were defined by Stein[16] as follows: For the *a*-axis,

$$f_a = (3\langle\overline{\cos^2\alpha}\rangle - 1)/2 \tag{4}$$

and, similarly, for the *b*-axis,

$$f_b = (3\langle\overline{\cos^2\beta}\rangle - 1)/2 \tag{5}$$

If the crystalline orientation in the filament is assumed to be cylindrically symmetrical with respect to the fiber axis, the average $\langle\cos^2\alpha\rangle$ and $\langle\cos^2\beta\rangle$ can be calculated from eqs. (6) and (7), respectively:

$$\langle\overline{\cos^2\alpha}\rangle = \frac{\int_0^{90} I_{200}(\Phi)\cos^2\Phi \sin\Phi \, d\Phi}{\int_0^{90} I_{200}(\Phi)\sin\Phi \, d\Phi} \tag{6}$$

$$\langle\overline{\cos^2\beta}\rangle = \frac{\int_0^{90} I_{020}(\Phi)\cos^2\Phi \sin\Phi \, d\Phi}{\int_0^{90} I_{020}(\Phi)\sin\Phi \, d\Phi} \tag{7}$$

where Φ is the azimuthal angle between the meridian and the reflection and $I_{200}(\Phi)$ and $I_{020}(\Phi)$ are the (200) and (020) intensities at the azimuthal angle Φ. The orientation function f_c for the *c*-axis (molecular axis) is calculated with eq. (8):

$$f_a + f_b + f_c = 0 \tag{8}$$

The long period of the as-spun fiber was investigated using small-angle X-ray scattering (SAXS) (Rigaku Co.).

Dynamic Viscoelasticity

The crystalline relaxation behavior was investigated using a Toyo Baldwin Rheovibron of DDV-II-C type in the temperature range of 20–120°C, at heating rate of 2°C/min and a frequency of 110 Hz.

Thermal Analysis

The thermal behavior of the HDPE fibers was investigated using a differential scanning calorimeter of Shimazu DSC-50. Thermal analysis of the 5-mg fiber sample was carried out from 25 to 200°C at the heating rate of 10°C/min. Heat shrinkage was measured by a thermal mechanical analyzer of Seiko TMA at the heating rate of 10°C/min and the initial load of 3 gf.

Table I Molecular Weight and Molecular Weight Distribution of HDPEs

Sample	$\bar{M}_n$	$\bar{M}_w$	MWD ($\bar{M}w/\bar{M}n$)
HDPE(11)	21,600	119,400	5.528
HDPE(28)	15,500	84,500	5.452

Tensile Property

Tensile properties of a 10-mm-long monofilament were measured using a Fafegraph-M tensile machine of Textecho Co. at a crosshead speed of 20 mm/min.

RESULTS AND DISCUSSION

Molecular Weight Distribution

The number-average molecular weight, weight-average molecular weight, and molecular weight distribution of HDPE polymers are shown in Table I. Average molecular weights of HDPE(11) are larger than those of HDPE(28), but the molecular weight distributions are almost the same.

Rheological Property

Figure 2 shows the changes of the dynamic shear viscosity with the frequency. It exhibits typical shear thinning. This phenomenon is due to the disentanglement and the partial orientation of the molecular chains. The viscosity of HDPE(28) is lower than that of HDPE(11) due to the difference of the MFRs between HDPE(11) and HDPE(28). The differences of the fiber-structure formation as well as spinnability are expected between HDPE(11) and HDPE(28).

Figures 3 and 4 show the storage modulus (G') and the loss modulus (G'') against the angular frequency, respectively. Both G' and G'' increase with increasing frequency, and those of HDPE(11) are larger than those of HDPE(28) owing to the lower MFR of HDPE(11). Tan δ versus frequency is plotted in Figure 5, where the tan δ of HDPE(28) is larger than that of HDPE(11). The result is due to the difference of the MFR between HDPE(11) and HDPE(28).

Molecular Orientation

The birefringence of the HDPE fibers is plotted against take-up velocity in Figure 6. With an increase in take-up velocity, the birefringence has shown a sigmoidal increase, which has distinct changes in the range of 1–5 km/min. It is due to the increase of stress in the spinline with increasing take-up velocity. Moreover, it shows that the birefringence changes gently at the take-up veloc-

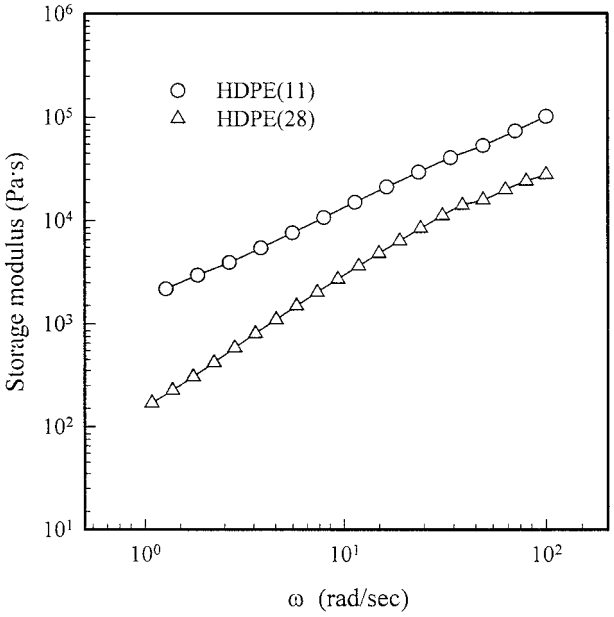

Figure 3 Storage modulus versus frequency for HDPE at 220°C.

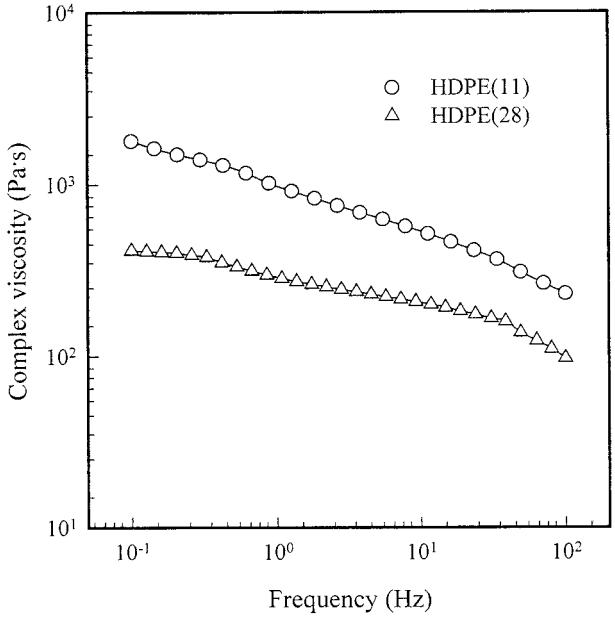

Figure 2 Complex viscosity versus frequency for HDPE at 220°C.

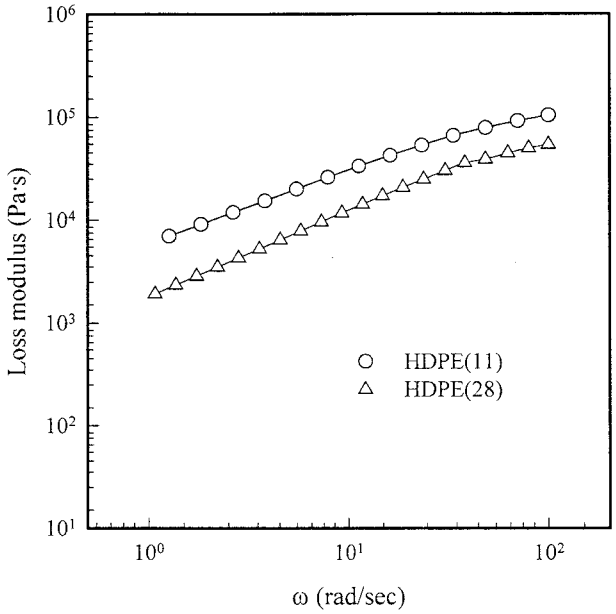

Figure 4 Loss modulus versus frequency for HDPE at 220°C.

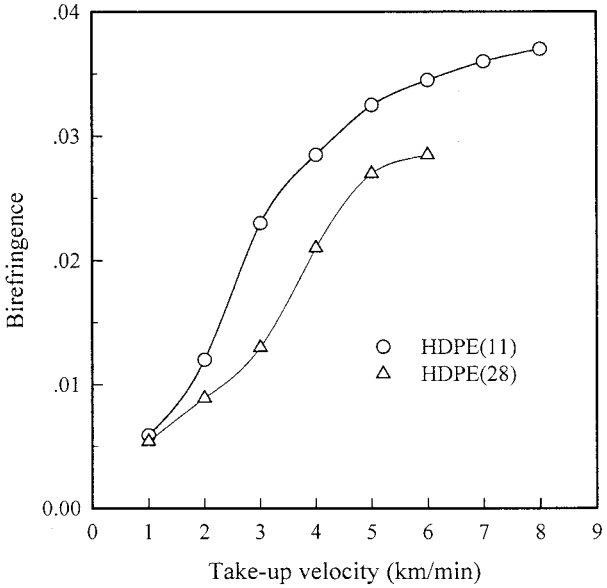

Figure 6 Relation between birefringence and take-up velocity for HDPE fibers.

ity of 6 km/min and above. The majority of molecules seem to be oriented near these take-up velocities. Throughout the whole range of take-up velocities, the birefringence of HDPE(11) was higher than that of HDPE(28). It seems that the molecular orientation of HDPE(11) gets better owing to larger extensional stress experienced in the spinline. This tendency was in accordance with the case of low-speed spinning by White,[13] that is, the increment of orientation due to higher molecular HDPE is affected by more spinline tension.

Figure 7 shows the density change with take-up velocity. The density of HDPE(28) was nearly

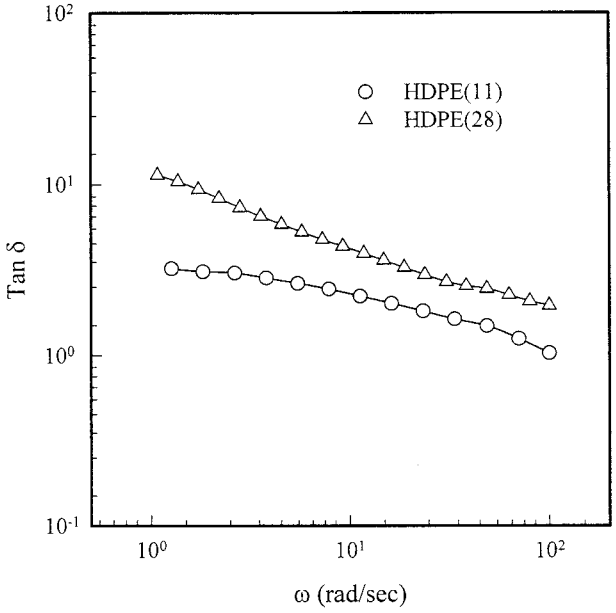

Figure 5 Tan δ versus frequency for HDPE at 220°C.

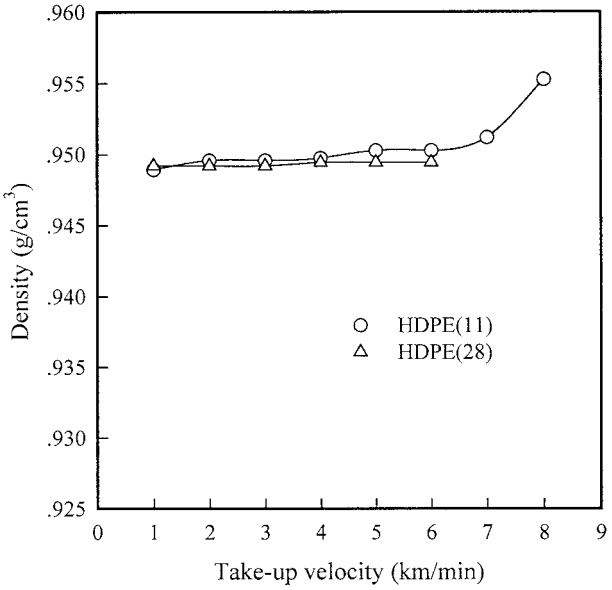

Figure 7 Relation between density and take-up velocity for HDPE fibers.

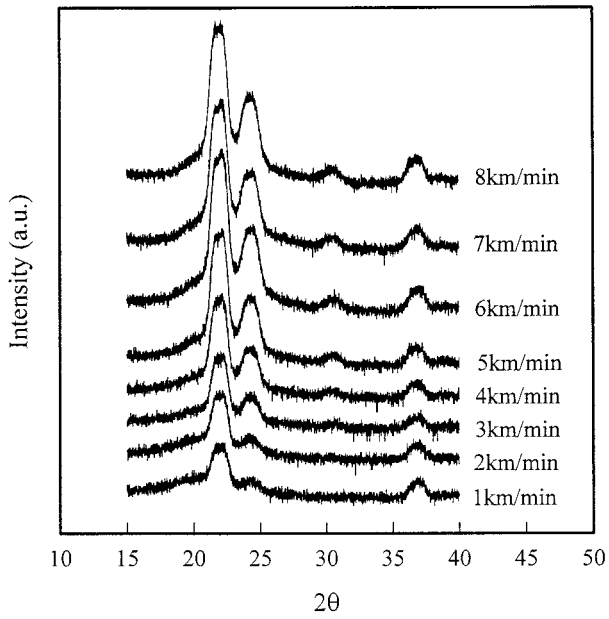

Figure 8 X-ray diffraction curves for HDPE(11) fibers according the various take-up velocities.

constant throughout the whole range of take-up velocities and that of HDPE(11) increased gently with the take-up velocity of up to 6 km/min, but at 5 km/min and above, the density increased sharply. It is supposed that the molecular orientation by spinline tension scarcely affects the density. Consequently, the fractions of crystalline and amorphous regions are nearly constant, independent of take-up velocity because of the rapid crystallization of HDPE itself. Compared to the birefringence, the molecular orientations of the crystalline and amorphous regions are influenced by the take-up velocity. For the case of HDPE(11), at a take-up velocity of 7 km/min and above, the density is increased by the orientation-induced crystallization with increasing take-up velocity. This tendency is because the effect of spinline tension is superior to that of the crystal formable rate in HDPE and then the fraction of the crystalline region is increased. Hence, it is possible to increase density by ultrahigh-speed spinning in spite of rapid crystallization of HDPE.

Analysis of Crystalline Structure

Figure 8 shows the wide-angle X-ray diffraction of melt-spun HDPE(11) fibers. HDPE exhibits the (110), (200), and (020) X-ray reflections at 2θ = 21.59, 24.03, and 36.30°, respectively. Crystal formation is realized at low-speed spinning and diffraction peaks become sharpened owing to rapid crystallization. Figure 9 shows the wide-angle X-ray diffraction of HDPE(28), which is similar to that of HDPE(11). The crystal formation in high-speed spinning seems to represent a tendency being irrelevant to the MFR of HDPE. A sharp crystalline peak of the HDPE(11) fiber spun at 8 km/min is closely related to the result of the density in Figure 7.

Figure 10 shows the crystallinity, calculated from the density, with the take-up velocity. The crystallinity of HDPE(28) is almost independent of the take-up velocity, but that of HDPE(11) increases gently to the take-up velocity of 6 km/min and remarkably above that. The above result means that the extensional stress affects the molecular orientation up to the take-up velocity of 6 km/min but affects, rarely, crystallinity because of the rapid crystallization HDPE. The molecular packing density increases with increasing extensional stress owing to the orientation-induced crystallization, at a take-up velocity of 7 km/min and above.

Figure 11 shows the azimuthal diffraction curves of (200) and (020) reflections for HDPE(11) spun at different take-up velocities. The (200) plane is oriented to the a-axis direction at the take-up velocity of 1 km/min, to lean 45° at 2 km/min, and to the c-axis orientation over 3 km/min, and then the orientation of the c-axis in-

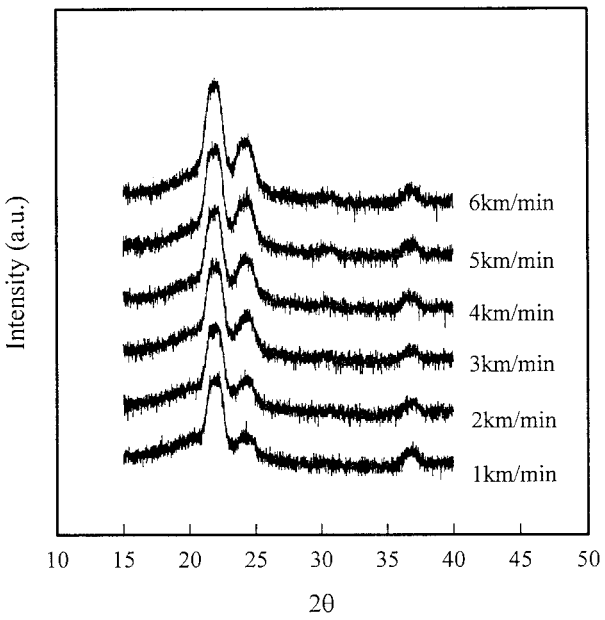

Figure 9 X-ray diffraction curves for HDPE(28) fibers according the various take-up velocities.

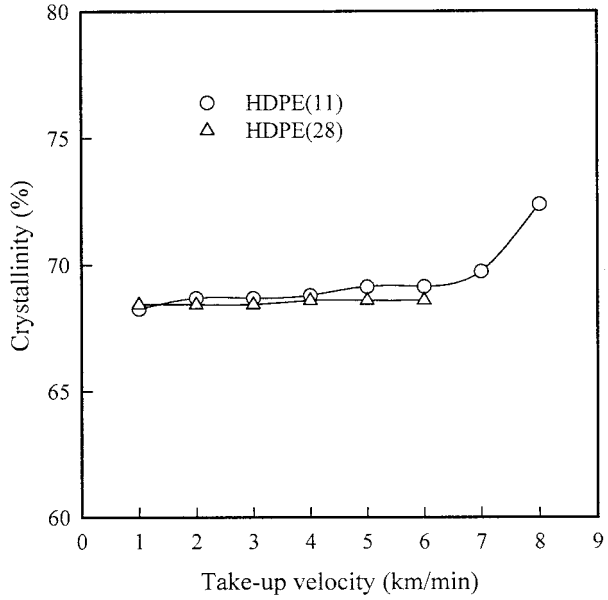

Figure 10 Relation between crystallinity and take-up velocity for HDPE fibers.

creases gradually with increasing take-up velocity. Hence, with increasing take-up velocity, the crystals are oriented to the fiber axis and the orientation of the crystal becomes higher. This phenomenon suggests that the crystals are oriented, with increasing take-up velocity, from the distorted lamellar structure to the undistorted lamellar structure and to the row-nucleated structure formed perpendicular to fiber axis, similarly to the low-speed spinning.[17] Figure 12 shows the azimuthal scans of (200) and (020) reflections for HDPE(28). Above the take-up velocity of 3 km/min, it has the orientation behavior of crystal like HDPE(11) but the degree of crystalline orientation is rather lower than that of HDPE(11). It seems that crystals are oriented to 45° against the fiber axis at the take-up velocity of from 2 to 3 km/min, compared to that of the HDPE(11), which is done at the take-up velocity of 2 km/min. Consequently, the crystalline orientation due to the take-up velocity has more effect on HDPE(11) than on HDPE(28).

Figure 13 shows the changes of the orientation function in the HDPE(11) fiber with the take-up velocity. With increasing take-up velocity, f_a and f_b decrease gradually and f_c increases. Figure 14 shows the orientation function of the HDPE(28) fiber spun at different velocities. f_a and f_b decrease and f_c increase with increasing take-up velocity. The f_c of HDPE(11) is higher than that of HDPE(28). It corresponds to the results of birefringence.

Figure 15 shows the meridional X-ray diffraction profile of HDPE(11) in the ranges of 2θ = 65–85°. The (002) plane is observed near 2θ = 75°, and the (202) plane, near 2θ = 80°. The (202) planes are oriented to 14.7° against the fiber axis. The oriented crystalline unit cell was shown to exist and was distributed in the take-up velocity range of 3–5 km/min. With increasing take-up velocity, the diffractive intensity of the (002) plane becomes larger and sharpened gradually, and at the take-up velocities of 7–8 km/min, the (200) plane has disappeared, meaning that the crystalline unit cell of HDPE(11) is oriented to the fiber axis at the higher take-up velocity. Figure 16 shows the meridional X-ray diffraction profile of HDPE(28). Up to the take-up velocity 6 km/min, the (202) plane was confirmed. It is because the crystalline unit cell is not oriented by the ultra-

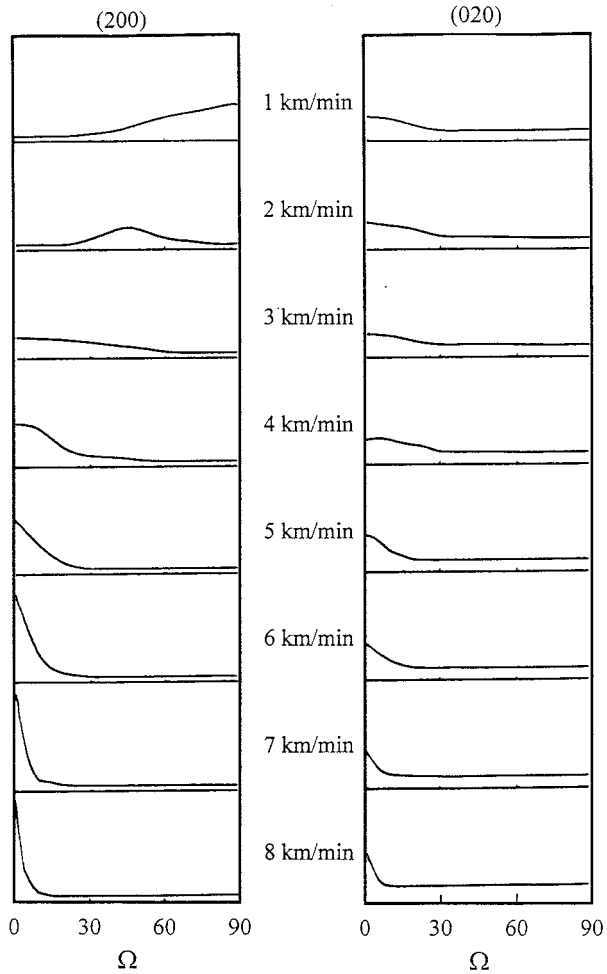

Figure 11 Variation of azimuthal profile of (200) and (020) intensities HDPE(11) as-spun fibers with the take-up velocity.

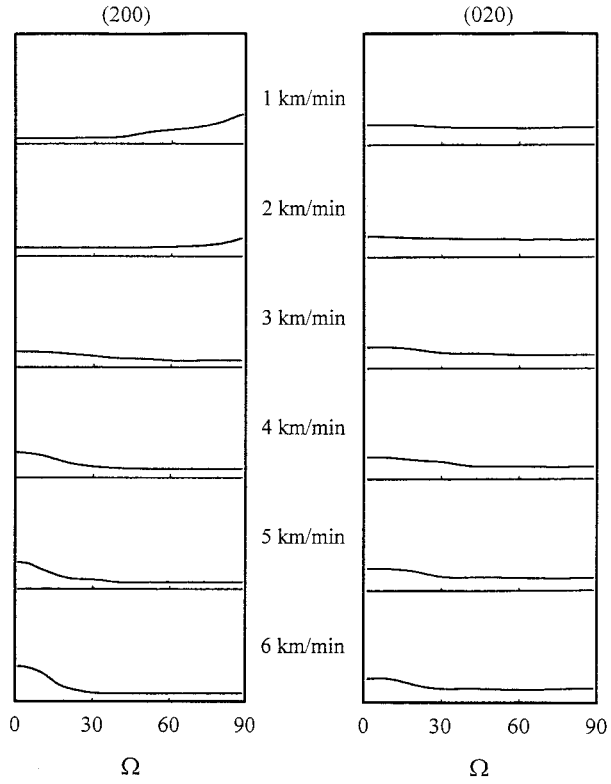

Figure 12 Variation of azimuthal profile of (200) and (020) intensities HDPE(28) as-spun fibers with take-up velocity.

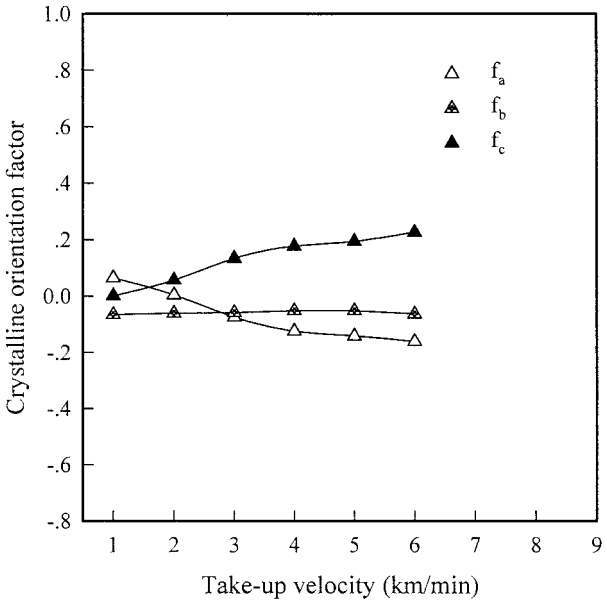

Figure 14 Crystalline orientation functions versus take-up velocity for HDPE(28).

high-speed spinning like HDPE(11) is. The difference between HDPE(11) and HDPE(28) in the orientation of the crystalline unit cell corresponds to the density results.

Figures 17 and 18 show the profile of small-angle X-ray diffraction. The structure of the long period was confirmed to be oriented, alterna-

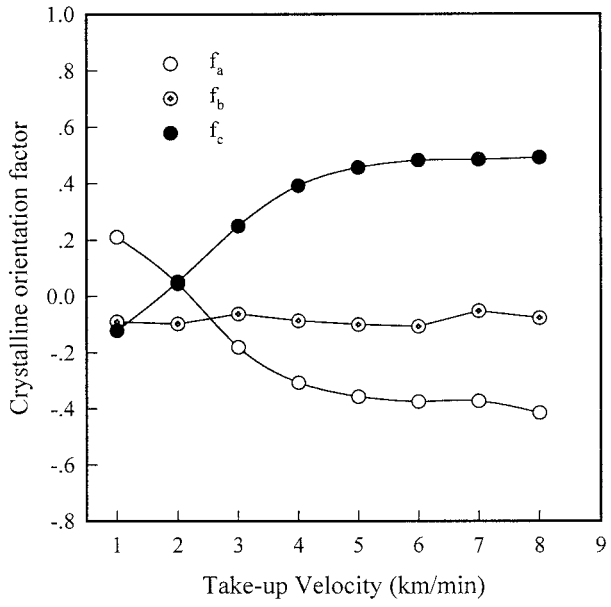

Figure 13 Crystalline orientation functions versus take-up velocity for HDPE(11).

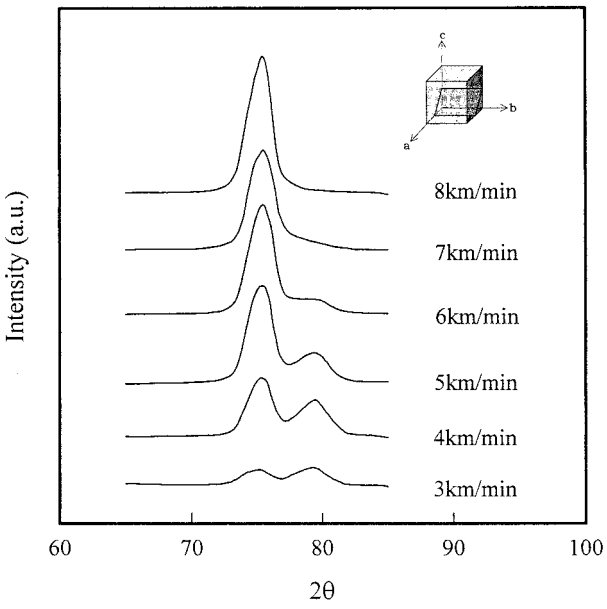

Figure 15 Wide-angle X-ray meridional scans of HDPE(11) fibers versus take-up velocity.

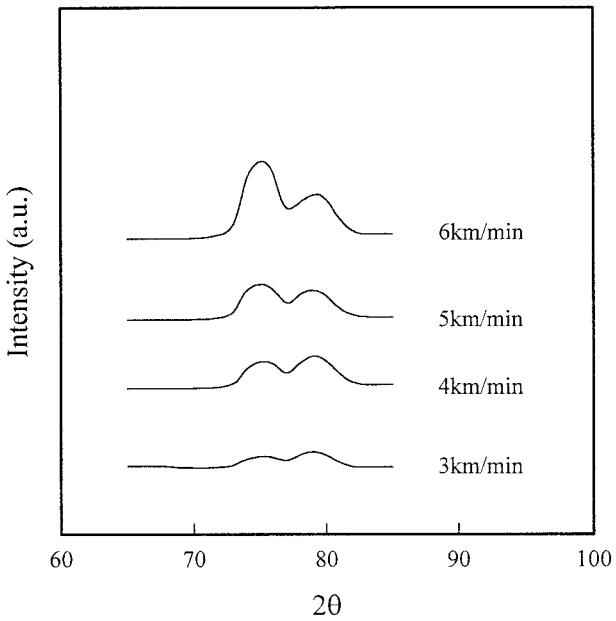

Figure 16 Wide-angle X-ray meridional scans of HDPE(28) fibers versus take-up velocity.

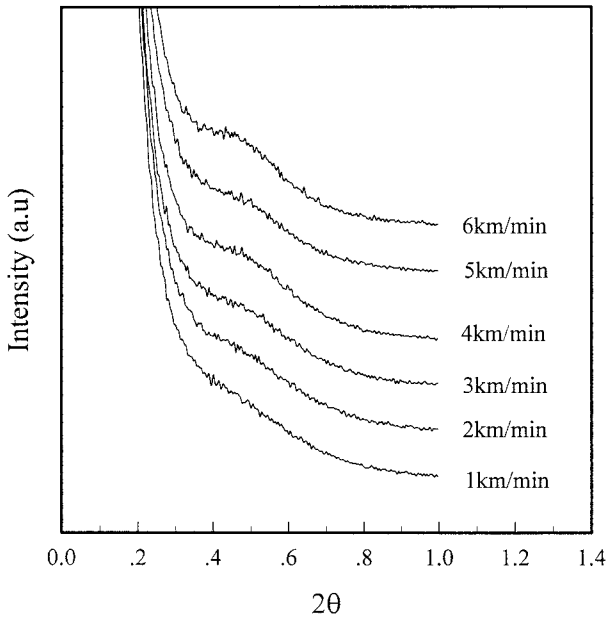

Figure 18 Changes of the SAXD meridional intensity curves of HDPE(28) fibers at various take-up velocities.

tively, crystalline and amorphous. The changes of long-periodal structure seem to be irrelevant to the take-up velocity.

Figure 19 shows the amorphous orientation factor (f_a) of the HDPE fibers. The amorphous orientation factor was calculated from eq. (9):

$$\Delta n = f_{cr}\Delta n^*_{cr}\chi_c + f_{am} \cdot \Delta n^*_{am}(1 - \chi_c) \qquad (9)$$

where Δn^*_{cr} (= 0.059) and Δn^*_{am} (= 0.28) are the intrinsic crystalline and amorphous birefringence, respectively.[18] With increasing take-up velocity, the orientation factor of HDPE(11) and HDPE(28) increases gradually and that of

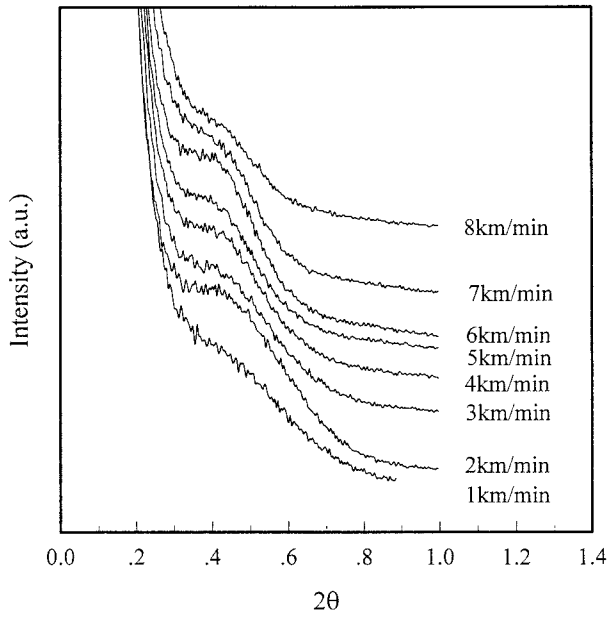

Figure 17 Changes of the SAXD meridional intensity curves of HDPE(11) fibers at various take-up velocities.

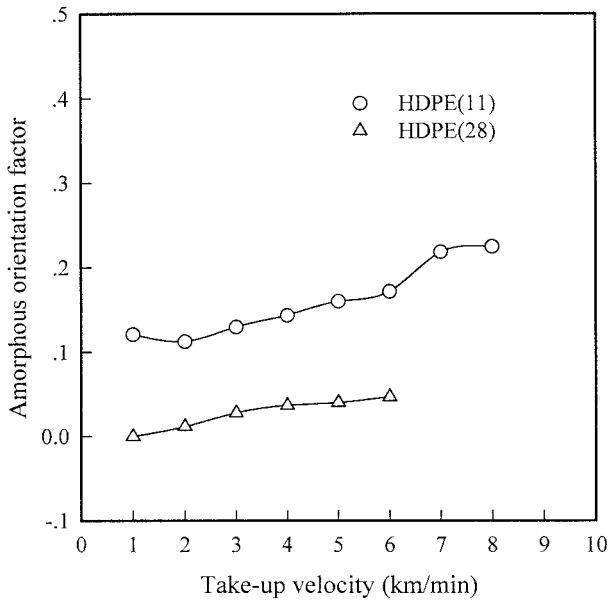

Figure 19 Relation between amorphous orientation factor and take-up velocity for HDPE fibers.

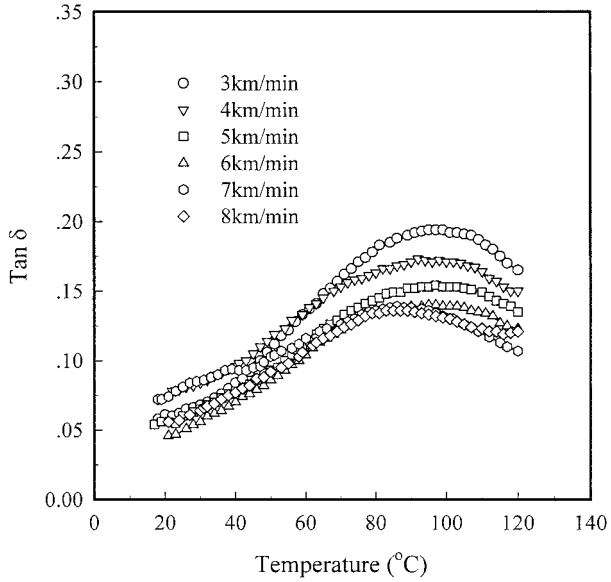

Figure 20 Tan δ values of HDPE(11) fibers versus take-up velocity.

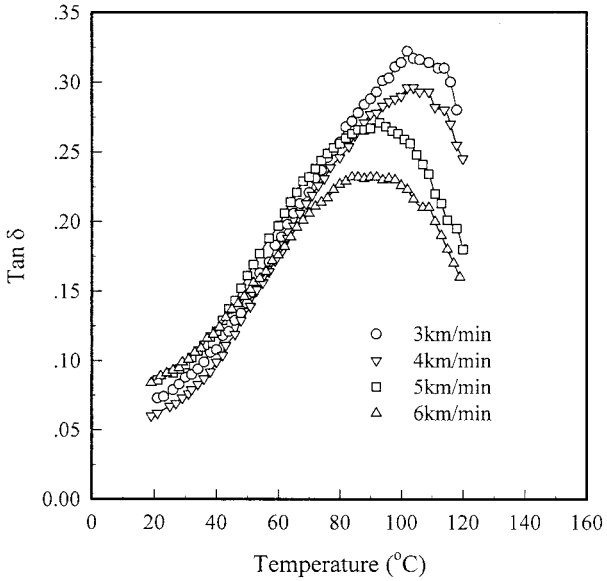

Figure 21 Tan δ values of HDPE(28) fibers versus take-up velocity.

HDPE(11) has the higher amorphous orientation factor, as in the birefringence results. In the case of HDPE(11), the amorphous orientation factor is increased suddenly at the take-up velocity of 7 km/min and above, as in the density results. These phenomena may affect the mechanical properties of HDPE fiber spun from high-speed spinning.

Behavior of Crystalline Relaxation

In general, the lamellar crystals formed from spherulites have defects in the crystal. Hence, although the central molecule formed a crystal, the molecular mobility in the crystal is mutually independent. This crystal is called a "plastic crystal."[19] As for the polymeric crystal, the plasticity between molecules in a crystal is caused by the noninterference lattice vibration, and, therefore, this is called "crystalline relaxation."[20–22] It is known that the crystalline relaxation is due to the vibration of chains inside a crystal (mainly, the rotational mobility around the *c*-axis) and the dispersion through the slippage of molecules in the crystal interface, the molecular mobility of lamellar surface, the rearrangement of defects in the crystal, and the complex interaction of the above reasons, but the exact reason and mechanism have been never investigated.

These crystalline relaxations are confirmed by the tan δ peak of high-speed spun HDPE fibers; the results of HDPE(11) and HDPE(28) are

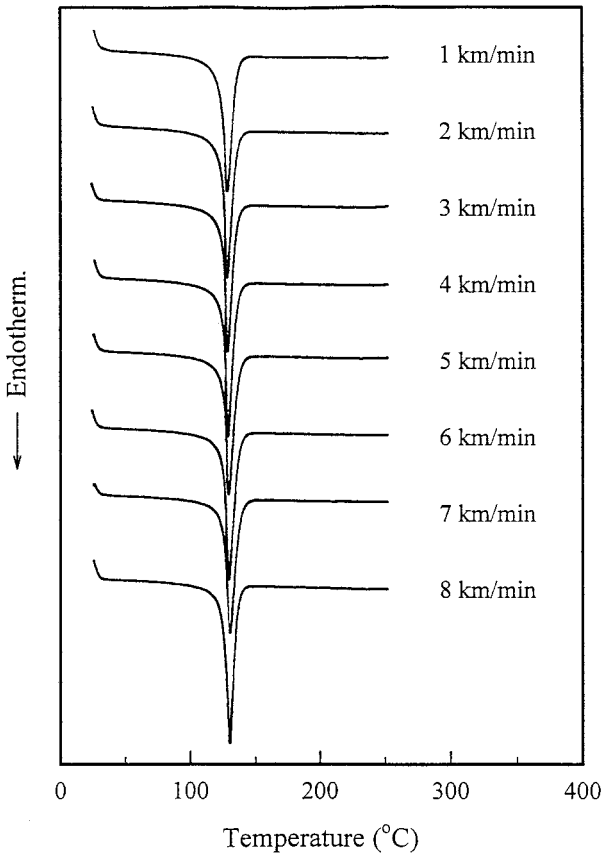

Figure 22 DSC thermograms for HDPE(11) fibers produced at various take-up velocities.

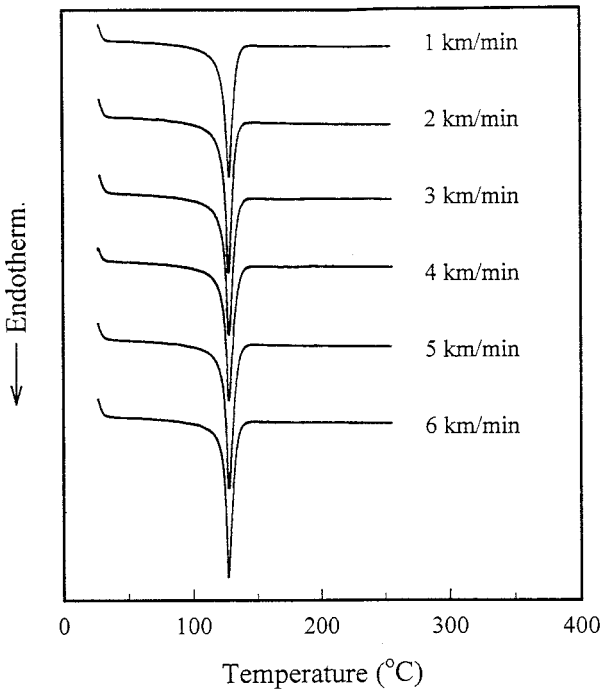

Figure 23 DSC thermograms for HDPE(28) fibers obtained at various take-up velocities.

shown in Figures 20 and 21, respectively. The intensity of the crystalline relaxation peak decreases with increasing take-up velocity in both HDPE(11) and HDPE(28). It is supposed that the fraction of defects in a crystal due to the compact structure decreases with increasing take-up velocity. It was shown that the peaks of the crystalline relaxation temperature were 25–45°C lower than the melting temperature. This phenomenon is due to the mobility of chains in the defects in crystals rather than the mobility of a perfect crystal. As above, the crystalline relaxation peaks shift to lower temperature with increasing take-

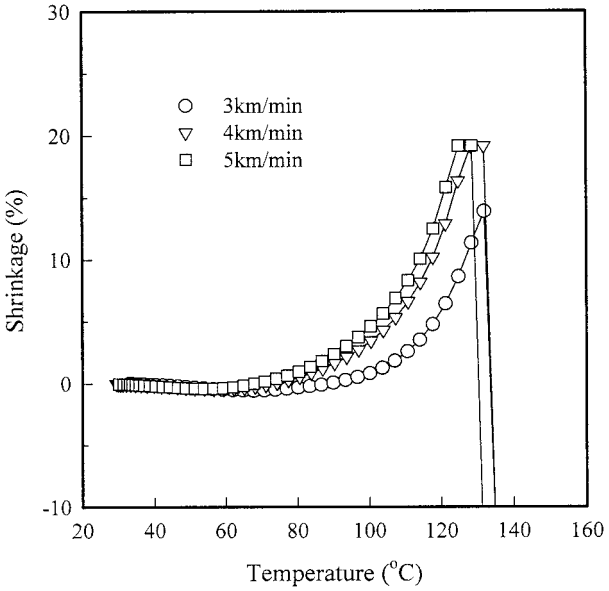

Figure 25 Shrinkage of HDPE(28) fibers during heat treatment versus take-up velocity.

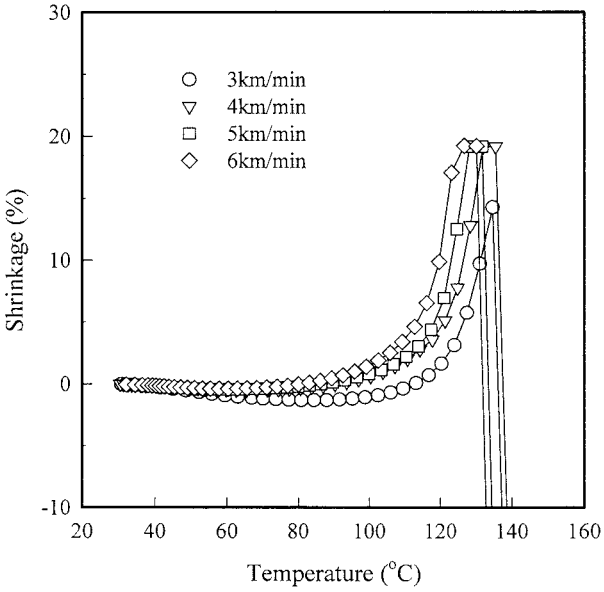

Figure 24 Shrinkage of HDPE(11) fibers during heat treatment versus take-up velocity.

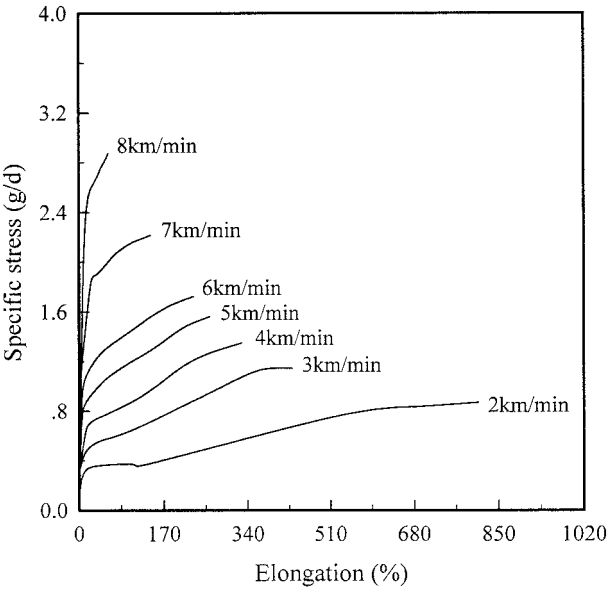

Figure 26 Stress–strain curves for HDPE(11) fibers obtained at various take-up velocities.

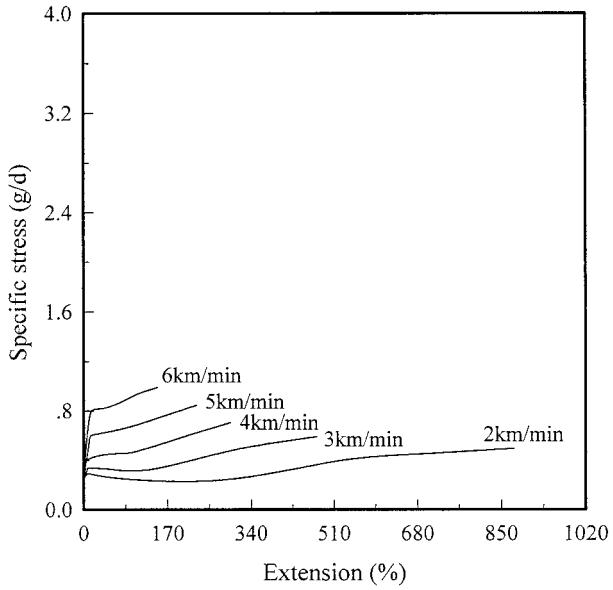

Figure 27 Stress–strain curves for HDPE(28) fibers obtained at various take-up velocities.

up velocity. The fraction of defects in a crystal decreases owing to a compactness of the crystalline structure, but the structure of defects comes to be more disentangled and the arrangement of defects in a crystal becomes more disentangled easily. The intensity of the crystalline relaxation of HDPE(11) is found to be lower than that of HDPE(28), and then it is supposed that the defects in a crystal of HDPE(11) are fewer than that of HDPE(28).

Thermal Property

Figures 22 and 23 show DSC thermograms of HDPE(11) and HDPE(28) fibers, respectively. It is supposed that HDPE fibers are crystallized independently of the take-up velocities because of rapid crystallization. The melting point, T_m, a measure of crystalline perfectness, remains nearly unchanged near 125–126°C throughout the whole range of take-up velocities. Therefore, it is guessed that the spinline tension on high-speed spinning hardly affects the perfectness of a crystal in HDPE fibers. For the case of HDPE(11), it is shown that the T_m increases about 1–2°C at the take-up velocity of 7 km/min and above. It is supposed that the packing of a crystal has been improved by the orientation-induced crystallization and a denser structure has been formed.

Figures 24 and 25 show the thermal shrinkage of HDPE(11) and HDPE(28) fibers produced at different take-up velocities. For both HDPE(11) and HDPE(28), it is shown that with increasing take-up velocity the onset point of shrinkage shifts lower, and then the degree of shrinkage becomes low and the extension near the melting temperature also becomes larger. This is probably because the relaxation of amorphous chains starts before melting and the quantity of relaxation on amorphous chains increases with increasing take-up velocity; therefore, with the higher-speed spinning, thermal shrinkage starts at the lower temperature. Consequently, with increasing take-up velocity, the generation of crimp caused by an elastic shrinkage immediately after spinning will be promoted and this effect is more detectable for HDPE(28) with a larger MFR.

Tensile Property

Figures 26 and 27 show the stress–strain curves of HDPE(11) and HDPE(28) fibers produced at different take-up velocities, respectively. The ini-

Table II Mechanical Properties of HDPE Fibers in High-Speed Spinning

Take-Up Velocity (km/min)	Initial Modulus (g/d)		Specific Stress (g/d)		Strain (%)		Work of Rupture (g × cm)	
	HDPE(11)	HDPE(28)	HDPE(11)	HDPE(28)	HDPE(11)	HDPE(28)	HDPE(11)	HDPE(28)
1	—	—	—	—	—	—	—	—
2	9.14	8.98	0.87	0.50	812.65	880.76	110.02	67.47
3	12.77	10.40	1.17	0.59	430.86	474.67	105.50	60.07
4	13.80	11.89	1.37	0.71	328.07	297.87	74.26	35.88
5	17.39	13.57	1.57	0.85	264.46	229.57	57.72	29.43
6	20.17	15.79	1.74	0.99	230.97	149.55	50.87	19.77
7	29.44		2.21		145.40		35.87	
8	40.61		2.87		60.24		18.18	

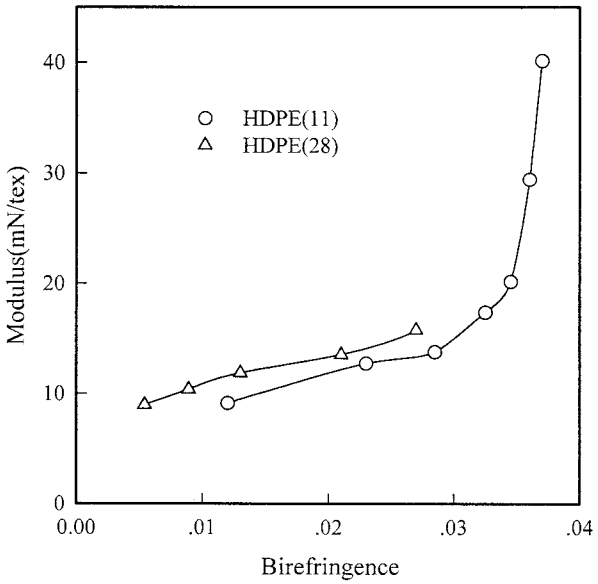

Figure 28 Modulus as a function of birefringence.

tial modulus, specific stress, extension, and work of rupture of the as-spun HDPE fibers are shown in Table II. It can be seen that the mechanical property is improved by high-speed spinning. The fibers spun at a take-up velocity of 1 km/min cannot observe the rupture because of the high elongation, and with increasing take-up velocity, the strain decreases but the tenacity and the initial modulus increase. The tendency was probably interpreted by the changes on the molecular orientation and fine structure, that is, the molecular orientation on HDPE fibers increases with take-up velocity. Compared with the physical properties between the HDPE(11) and HDPE(28) fibers, HDPE(11) with a higher molecular orientation shows better mechanical properties.

Figure 28 shows plots of tenacity versus birefringence, and this shows good correlation. It is supposed that the tenacity increases due to the increases of the molecular orientation. Consequently, in spite of the rapid crystallization of HDPE, it exhibits an improved mechanical property by the ultrahigh-spinning.

CONCLUSIONS

High-speed spinning of HDPE(11) and HDPE(28) was carried out and the fiber-structure formation and the physical properties were investigated by birefringence, wide-angle X-ray diffraction, thermal analysis, the tensile test, etc.:

1. HDPE(11) is superior to HDPE(28) in fiber-structure formation as well as spinnability.
2. The birefringence of HDPE fibers showed a sigmoidal-type increase with increasing take-up velocity.
3. The crystalline orientation was transformed from *a*-axis orientation to *c*-axis orientation with increasing take-up velocity.
4. Crystalline relaxation was observed in the temperature range of 25–45°C lower than the melting temperature. The intensity of the crystalline relaxation peak decreased and the peak temperature shifted lower with increasing take-up velocity.

REFERENCES

1. Ueda, S.; Ogawa, N.; Hasegawa, S.; Kitajima, F.; Fujimoto, S.; Kanetsuna, H.; Kurita, T. Presented at the meeting of the Research Institute for Polymers and Textiles in Japan, 1971.
2. Shimizu, J.; Toriumi, K.; Imai, Y. Sen'i Gakkaishi 1977, 33, T-255.
3. Shimizu, J.; Okui, N.; Imai, Y. Sen'i Gakkaishi 1979, 35, T-405.
4. Shimizu, J.; Okui, N.; Imai, Y. Sen'i Gakkaishi 1980, 36, T-166.
5. Shimizu, J.; Okui, N.; Kikutani, T.; Ono, A.; Takaku, A. Sen'i Gakkaishi 1981, 37, T-143.
6. Shimizu, J.; Toriumi, K.; Tamai, K. Sen'i Gakkaishi 1977, 33, T-280.
7. Shimizu, J.; Okui, N.; Kaneko, A.; Toriumi, K. Sen'i Gakkaishi 1978, 34, T-64.
8. Shimizu, J.; Okui, N.; Kikutani, T.; Toriumi, K. Sen'i Gakkaishi 1978, 34, T-93.
9. Heuvel, H. M.; Huisman, R. J Appl Polym Sci 1978, 22, 2229.
10. Jacob, I.; Schöder, H. R. Chemiefasern/Textilind 1980, 30, 114.
11. Shimizu, J.; Okui, N.; Imai, Y. Sen'i Gakkaishi 1979, 35, T-405.
12. Ziabicki, A.; Kawai, H. High-Speed Fiber Spinning; Wiley: New York, 1985; Chapter 15.
13. White, J. L. J Appl Polym Sci 1964, 8, 2339.
14. Dees, J. R.; Spruiell, J. E. J Appl Polym Sci 1974, 18, 1053.
15. Beret, S.; Prausnitz, J. M. Macromolecules 1975, 8, 536.
16. Stein, R. S. J Polym Sci 1959, 34, 709.
17. Kitao, T.; Ohya, S.; Furukawa, J.; Yamashita, S. J Polym Sci Polym Phys 1973, 11, 1091.
18. Boenig, H. V. Polyolefins: Structure and Properties; Elsevier: Amsterdam, 1966.
19. Iwayanagi, S.; Miura, I. Jpn J Appl Phys 1965, 4, 94.
20. Sinnott, K. M. J Appl Phys 1966, 37, 3385.
21. Takayanagi, M.; Matsuo, T. J Macromol Sci-Phys B 1967, 1, 407.
22. Sinnott, K. M. J Polym Sci C 1966, 14, 141.